CELL CYCLE
2020, VOL. 19, NO. 5, 551–566
https://doi.org/10.1080/15384101.2020.1717043

Taylor & Francis
Taylor & Francis Group

RESEARCH PAPER

The protective effects of microRNA-26a in steroid-induced osteonecrosis of the femoral head by repressing EZH2

Gang Li[a#], Haifeng Liu[a#], Xiaogang Zhang[a], Xingchao Liu[a], Guodong Zhang[a], and Qinghe Liu[b]

[a]Department of Orthopedics, Hebei Yanda Hospital, Hebei Medical University, Sanhe, China; [b]Department of Orthopedics, Beijing Chaoyang Hospital, Capital Medical University, Beijing, China

ABSTRACT

Recently, the role of microRNAs (miRs) in human diseases has been verified. This study was determined to explore the protective effects of microRNA-26a (miR-26a) in steroid-induced osteonecrosis of the femoral head (SONFH) with the involvement of enhancer of zeste homologue 2 (EZH2).

Femoral head (FH) samples from SONFH patients and patients with femoral neck fracture were collected, and rat SONFH models were established by Escherichia coli endotoxin combining with large dose steroid pulse assay. The hemorheology, blood lipid, inflammatory factors, and pathologic changes were measured by a series of experiments. Moreover, the detection of osteoblasts, osteoclasts, miR-26a expression, EZH2 expression, osteoprotegerin (OPG) and osteoprotegerin ligand (OPGL), and the apoptosis of osteocytes were conducted. The target relation between miR-26a and EZH2 was clarified by bioinformatics and dual-luciferase reporter gene assay.

MiR-26a was poorly expressed, while EZH2 was highly expressed in SONFH, and the elevation of miR-26a could repress EZH2 expression. Elevated miR-26a and reduced EZH2 were able to decelerate the apoptosis of osteocytes, increase osteoblasts, and decrease osteoclasts, resulting in a repression of SONFH progression. Additionally, EZH2 was a target gene of miR-26a. Furthermore, the elevation of EZH2 could reverse the repression of SONFH progression that is induced by elevated miR-26a.

We found that up-regulation of miR-26a and knockdown of EZH2 could suppress the development of SONFH, which would contribute to the therapy of SONFH.

ARTICLE HISTORY
Received 19 September 2019
Revised 8 December 2019
Accepted 29 December 2019

KEYWORDS
Steroid-induced osteonecrosis of the femoral head; microRNA-26a; enhancer of zeste homologue 2; apoptosis; osteoblast; osteoclast

Introduction

Osteonecrosis of the femoral head (ONFH) is an orthopedic disease that necrotic bone injuries often developed to lacunae of femoral head (FH) and symptomatic hip osteoarthritis [1]. ONFH can be separated into traumatic and non-traumatic ONFH [2]. As a subtype of non-traumatic ONFH, steroid-induced ONFH (SONFH) is correlated with the elevation of pressure in bone that was resulted from increased lipogenesis and hyperplasia of adipocytes in bone marrow, which could decelerate the blood flow in FH and eventually cause avascular osteonecrosis [3]. According to the statistics, there were 150,000–200,000 patients newly diagnosed with ONFH every year in China until 2017 [4], and SONFH was diagnosed in 24.1% of the ONFH patients [5]. The incidence of SONFH is correlated with the management methods and the dose of the steroid. Moreover, SONFH usually could not be early diagnosed for most patients [6]. Resulted from non-specific symptom in the early period, patients with SONFH usually miss the best time to receive non-surgical therapy, hence early diagnosis and therapy of SONFH remain significant [7]. Therefore, it is essential to explore novel treatments of SONFH.

Non-coding small RNAs are also known as microRNAs (miRNAs), which usually include about 20 nucleotides and have the capacity to regulate some target genes [8]. In recent decades, a number of miRNAs have been confirmed and characterized in human diseases, and there were many researchers who have proven that miRNAs were related to the development of SONFH, such as miR-708 [9] and miR-27a [10]. As one of the miRNAs, miR-26a was found to be associated with several kinds of human diseases, such as osteosarcoma [11,12], bone trauma [13] and

CONTACT QingHe Liu Liuqinghe2019@163.com
[#]These authors are co-first authors.

osteoarthritis of knee joints [14]. Moreover, enhancer of zeste homologue 2 (EZH2) is a catalytic subunit of polycomb repressive complex 2, which is implicated in restraining the expression of gene by methylated histone H3 on lysine 27 [15]. According to the previous studies, EZH2 was correlated with osteosarcoma [16,17] and multiple myeloma [18]. In addition, the correlation between miR-26a and EZH2 has been reported in multiple studies, for example, the double-negative feedback loop between EZH2 and miR-26a has been demonstrated to be able to modulate the development of hepatocellular carcinoma [19]. Furthermore, miR-26a could act as an inhibitor of nasopharyngeal carcinoma via reducing EZH2 [20]. Nevertheless, the combined impacts of miR-26 and EZH2 on SONFH remain unknown, hence our research was focused on the effects of miR-26a and EZH2 in the procedures of SONFH, and we speculated that miR-26a may function as a protective part in SONFH by targeting EZH2.

Materials and methods

Ethics statement

Written informed consents were obtained from all patients prior to the study. The protocols of this study were approved by the Ethics Committee of Beijing Chaoyang Hospital, Capital Medical University and based on the ethical principles for medical research involving human subjects of the *Declaration of Helsinki*. Animal experiments were strictly in accordance with the Guide to the Management and Use of Laboratory Animals issued by the National Institutes of Health. The protocol of animal experiments was approved by the Institutional Animal Care and Use Committee of Beijing Chaoyang Hospital, Capital Medical University.

Study subjects

A number of 52 FH specimens form SONFH patients (32 males and 20 females, aged 46.6 ± 14.3 years, weighed 56.3 ± 4.8 kg) that treated in bone and joint surgery of Beijing Chaoyang Hospital, Capital Medical University from December 2015 to January 2018 were collected as the SONFH group. An amount of 30 FH specimens from patients with femoral neck fracture (FNF) that received total hip replacement (18 males and 12 females, aged 49.6 ± 13.3 years, weighed 51.0 ± 6.2 kg) were selected as the control group. There were no evident differences in the gender, age, and body mass index among the patients in the two groups ($P > 0.05$).

Experimental animals

Ninety-six male Sprague Dawley (SD) rats (aged 8 w, weighed 200 ± 30 g) were obtained from Hunan SLAC Laboratory Animal Co., Ltd. (Changsha, China). Feeding conditions: temperature at 22-26°C, relative humidity at 37-42%, air was changed 15–20 times/h, illumination intensity at 150–200 Lx, 12 h day/night cycle, noise < 50 dB, six rats in one cage, and the rats were given free access to food and water.

Establishment of rat models

Except for the control group, rats in other groups were made into SONFH models [21]: the rats were conducted with intraperitoneal injection of Escherichia coli endotoxin (20 μg/kg) twice, 24 h/time. Then, the rats were conducted with intramuscular injection of methylprednisolone sodium succinate (40 mg/kg) through gluteus for three times, 24 h/time. Rats in the control group were injected with same volume of normal saline. With the successful establishment of the models, the mental state, activity, diet, temperature changes, weight changes, urination and defecation, and deaths of the rats were observed.

Animal grouping

After acclimated for 2 w, the successfully modeled 96 SD rats were separated into 8 groups (12 rats in each group). The normal group: no special treatment; the model group: SONFH models were established by Escherichia coli endotoxin combined high dose steroid, and each rat was intramuscularly injected with 2 mL normal saline on the 1st, 3rd, and 6th week of the experiment; the agomir negative control (NC) group: SONFH rats were injected with NC of adenovirus vector overexpressing miR-26a on the 1st, 3rd, and 6th week of the experiment ; the miR-26a agomir group: SONFH rats were injected with adenovirus vector overexpressing miR-26a on the 1st, 3rd, and

6th week of the experiment; the si-NC group: SONFH rats were injected with NC of adenovirus vector silencing EZH2 on the 1st, 3rd, and 6th week of the experiment; the si-EZH2 group: SONFH rats were injected with adenovirus vector silencing EZH2 on the 1st, 3rd, and 6th week of the experiment; the miR-26a agomir + oe-NC group: SONFH rats were injected with adenovirus vector overexpressing miR-26a and NC of adenovirus vector overexpressing EZH2 on the 1st, 3rd, and 6th week of the experiment; the miR-26a agomir + oe-EZH2 group: SONFH rats were injected with adenovirus vector overexpressing miR-26a and adenovirus vector overexpressing EZH2 on the 1st, 3rd, and 6th week of the experiment. Eight weeks after the experiment, fasting arterial blood (5 mL) from rats in each group was conducted with hemorheology, blood lipid, and inflammatory factor detection. Then, the rats were euthanized with their FHs extracted, the FHs were splitted along the coronal planes and the morphology of the FHs was observed. Subsequently, the bone tissues were sectioned for subsequent experiments.

Detection of blood indices

Hemorheology determination: the blood collected after the 8th week was conducted with the detection of the viscosity of whole blood at low and high shear, plasma viscosity, and hematocrit by LBY-N6B fully automatic modular hemo rheometer (Precil Instrument Co., Ltd., Beijing, China).

Blood lipid examination: the blood collected after the 8th week was centrifuged at 3500 rpm and 4°C for 15 min, the serum was extracted and preserved at 4°C, then conducted with the detection of total cholesterol (CHO), triglyceride (TG), and very low-density lipoprotein (vLDL).

Detection of inflammatory factors interleukin 6 (IL-6), tumor necrosis factor-α (TNF-α), and IL-1β: the collected blood was placed at 4°C for 4 h and centrifuged at 7200 r/min for 15 min with the serum collected, the changes of levels of IL-6, TNF-α and IL-1β in the serum were evaluated by enzyme-linked immunosorbent assay (all the kits were acquired from R&D Systems, Minneapolis, MN, USA). Next, standard solution (50 μL) was, respectively, added into blank microwells according to the order of standards, and the blank wells were appended with 50 μL sample, blank control wells were supplemented with 50 μL phosphate-buffered saline (PBS, pH 7.0–7.2), and each well was added with 100 μL enzyme-labeled solution (blank control wells were excluded). Subsequently, the plates were incubated at 37°C for 1 h. After washed for 5 times (the concentrate cleaning solution was diluted by distilled water at 1: 100), each well was appended with 50 μL developer A and 50 μL developer B, then reacted at 37°C without light exposure for 10–15 min. The reaction was stopped by adding 50 μL stop buffer in each well, and absorbance (A) value was measured by a microplate reader, which was converted into concentration unit.

Hematoxylin-eosin (HE) staining

The bone tissue specimens were fixed in 10% neutral buffered formalin for 24 h and decalcified by 5% ethylene diamine tetraacetic acid (EDTA) for 4 w, and the solution was changed every 3 d. The specimens of the SONFH group and the control group were dehydrated by gradient ethanol (70%, 80%, 90%, 95%, and 100%), permeabilized twice by xylene, 5 min/time, then embedded by paraffin and sectioned into 4 μm (part of the sections were prepared for the immunohistochemical staining). After toasted at 80°C for 1 h, the sections were dehydrated by gradient ethanol, permeabilized by xylene and stained by hematoxylin for 4 min, then the sections were differentiated by hydrochloric alcohol for 10 s, blued by ammonium hydroxide for 10 min, and stained by eosin for 4 min. Next, the sections were dehydrated by gradient ethanol, 1 min/time, permeabilized by xylene twice, 1 min/time, and the sections were sealed by neutral balsam, then the differences in cell morphology of FHs in the SONFH group and the control group were observed under a light microscope.

HE staining of animal experiment was the same with above steps, the pathological changes of ONFH tissues were observed by a light microscope, the rate and area of bone lacuna of the sections were measured using an image analyzer (× 40), and the area of trabeculae was also evaluated (× 10). Three fields of view were selected from each section, and the mean value was calculated.

Immunohistochemical staining

The sections were toasted at 60°C for 1 h, dewaxed by xylene, dehydrated by gradient ethanol, and

rinsed by PBS for three times, 5 min/time. Next, the sections were soaked in 3% H_2O_2 for 10 min inactivation of endogenous enzymes, washed by distilled water for 3 times, then added with 0.01 M citric acid buffer (pH = 6.0) and heated in a microwave. After appended with 5% bovine serum albumin (BSA) for 20 min, the sections were then supplemented with primary antibodies EZH2 (1:1000, Cell Signaling Technologies, Beverly, MA, USA), osteoprotegerin (OPG, 1:100) and osteoprotegerin ligand (OPGL, 1:100, both from Abcam Inc., Cambridge, MA, USA) at 4°C overnight. Subsequently, the sections were added with horseradish peroxidase (HRP)-labeled secondary antibodies at 37°C for 30-min incubation, appended with streptavidin-biotin complex at 37°C for 20 min, and developed by diaminobenzidine (DAB). The sections were counterstained by hematoxylin, soaked in 70%, 80%, 90%, 95% ethanol and absolute ethanol, each for 5 min, then dehydrated and permeabilized by xylene, and sealed by neutral balsam. Replacing primary antibody, PBS was taken as the NC. Five fields of view in each section were selected under a light microscope, the positive rate was calculated as the rate of brown positive particles.

Electron microscope observation

The sections were decalcified by 2.5% EDTA for 1.5 h, pre-fixed by 2.5% glutaraldehyde for 1.5 h, and after-fixed by 1% osmic acid for 1.5 h. Then, the sections were dehydrated successively with double distilled water, 30% ethanol, 50% ethanol (each for 5 min), 70% ethanol (10 min), 90% ethanol (twice, 10 min/time), and absolute acetone (3 times, 10 min/time). Next, the sections were soaked in mixed solution (absolute acetone: embedding reagent = 1:1) for 1 h and solution containing absolute acetone and embedding reagent at 1:2 for 4 h. After immersed in embedding reagent for 3 min, the sections were toasted at 37°C for 12 h and at 60°C for 36 h, then double stained by uranyl acetate and lead citrate. The changes of osteocytes of the FHs were observed by a transmission electron microscope.

Alkaline phosphatase (ALP) staining

Brownish or red particles could be found in the cytoplasm of the mature osteocytes after the sections were conducted with ALP staining according to the instructions of ALP kits (NanJing JianCheng Bioengineering Institute, Nanjing, China). The sections were dewaxed by xylene I and xylene II, each for 15 min, and successively soaked in absolute ethanol I, absolute ethanol II, 95%, 95%, 90%, 80%, and 75% ethanol, each for 5 min, then rinsed by tri-distilled water for 3 times, 2 min/time, and added with medium at 37°C without light exposure for 15-min incubation. Next, the sections were immediately stained with dye liquor for several times. The sections were then photographed by a light microscope (200 ×), the number of osteoblasts was counted by an image analyzer (Image-Proplus 6.0).

Tartrate resistant acid phosphatase (TRAP) staining

The mature osteoclasts were in purplish-red after stained by TRAP kits (Sigma-Aldrich Chemical Company, St Louis, MO, USA) according to the directions. The sections were dewaxed by xylene I and xylene II, each for 15 min, and successively soaked in absolute ethanol I, absolute ethanol II, 95%, 95%, 90%, 80%, and 75% ethanol, each for 5 min, then rinsed by tri-distilled water for 3 times, 2 min/time, then fixed by fixative solution for 30 s. Subsequently, the sections were placed in TRAP and incubated at 37°C for 1 h, counterstained by hematoxylin for 2 min and washed by tap water for 3 min. The sections were then photographed by a light microscope (200 ×), the number of osteoclasts was counted by Image-Proplus 6.0.

Terminal deoxynucleotidyl transferase-mediated dUTP nick end-labeling (TUNEL) staining

The FH sections were dewaxed and detached by pepsin (pH = 2) at 37°C for 30 min, each section was added with 50 μL TUNEL reaction solution (5 μL terminal deoxynucleotidyl transferase and 45 μL labeling solution) at 37°C for 60-min incubation, and added with 50 μL anti-fluoresceine isothiocyanate (FITC)-ALP antibody at 37°C for 30-min incubation. Next, each section was appended with 50 μL pleurotus citrinopileatus protein/nitroblue tetrazolium (PCIP/NBT) for 15 min, counterstained by nuclear fast red, and sealed by aqueous mounting media. The apoptosis was observed under a light microscope; nuclei stained into black-blue were

positive. Three fields of view were randomly elected from each section, and the rate of apoptotic cells in half of the fields of view was measured, then the sections were photographed. The TUNEL kits were obtained from Roche Ltd. (Basel, Switzerland).

Reverse transcription quantitative polymerase chain reaction (RT-qPCR)

The total RNA in bone tissues was extracted by Trizol kits (Invitrogen Inc., Carlsbad, CA, USA) and the concentration was evaluated by an ultraviolet spectrophotometer, the quality of total RNA was determined by agarose electrophoresis. The RNA was reversely transcripted into cDNA by RT kits (Sigma-Aldrich Chemical Company, St Louis, MO, USA) according to the instructions. The primers were designed and synthesized by Invitrogen Inc. (Carlsbad, CA, USA) and Takara Biotechnology Ltd. (Dalian, China) (Table 1). Glyceraldehyde phosphate dehydrogenase (GAPDH) was taken as the internal reference of EZH2 and U6 was taken as the internal reference of miR-26a. The data were analyzed by $2^{-\Delta\Delta Ct}$ method.

Western blot analysis

The total protein in the bone tissues was extracted by radio-immunoprecipitation assay, the protein concentration was measured under the guide of the directions of bicinchoninic acid kits (BOSTER Biological Technology Co., Ltd., Wuhan, Hubei, China). The extracted proteins were added with buffer solution and boiled at 95°C for 10 min, each well was added by 30 μg sample, and the proteins were conducted with 10% polyacrylamide gel electrophoresis, which were transferred onto the polyvinylidene fluoride membranes, and added with 5% BSA for 1 h. Next, the membranes were supplemented with primary antibodies EZH2, GAPDH (1: 1000, both from Cell Signaling Technology, Beverly, MA, USA), Bcl-2 and Bax (1: 500, both from Santa Cruz Biotechnology, Inc, Santa Cruz, CA, USA) at 4°C overnight. The membranes were then rinsed by tris buffer solution with tween (TBST) for 3 times, 5 min/time, and added with goat anti-rabbit HRP-labeled secondary antibody (Miaotong biological technology Co., Ltd., Shanghai, China) for 4-h incubation. After washed by TBST (3 times, 10 min/time), the membranes were developed by chemiluminescence reagent. GAPDH was taken as the internal reference, the gray value of each band was determined by CDC-8000 gel imaging analysis system. The ratio of gray value was taken as the relative expression of the proteins.

Table 1. Primer sequence.

Gene	Primer
GAPDH	F: 5′-CCACTCCTCCACCTTTGAC-3′
	R: 5′-ACCCTGTTGCTGTAGCCA-3′
EZH2	F: 5′-AGGGAAGAGGAGGAGATGAG-3′
	R: 5′-GCTGGGTTTGTCGGTGTT-3′
U6	F: 5′-CGGGCTGATGTACCAGTTCT-3′
	R: 5′-AACGCCTTCACGAATTTGCGT-3′
miR-26a	F: 5′-GGATCCGCAGAAACTCCAGAGA-3′
	R: 5′-TTGGAGGAAAGACGATTTCCGT-3′

Notes: F, forward; R, reverse; GAPDH, glyceraldehyde phosphate dehydrogenase; EZH2, enhancer of zeste homologue 2; miR-26a, microRNA-26a.

Dual-luciferase reporter gene assay

The target relation between miR-26a and EZH2, and binding sites of miR-26a and EZH2 3′-untranslated region (3′UTR) were predicted by bioinformatics software (http://www.targetscan.org). The EZH2 3′UTR wild type (WT) and mutant type (MUT) amplimers containing the binding sites were, respectively, designed, which were conducted with gel extraction purification. The recycling products were connected with pGEM-T vector and transferred into Top 10 competent bacteria by T ligase, thereby the recons were screened and identified. According to the protocols of plasmid extraction kits (Invitrogen Inc., Carlsbad, CA, USA), the WT and MUT recombinant pGEM-T plasmids were extracted and double-digested by restriction enzymes Xba I and Xho I, and the products were purified and recycled. Next, the plasmids were connected with luciferase reporter vector pmir-GLO (Promega Corporation, Madison, WI, USA) by T4DNA ligase, then transformed to DH5α competent Escherichia coli. After extracted, the plasmids were identified and sequenced by double digestion of Xbal and Xhol. The recombinant plasmids were, respectively, named as EZH2-3′UTR-WT and EZH2-3′UTR-MUT plasmids. Then, EZH2-3′UTR-WT and EZH2-3′UTR-MUT plasmids were co-transfected into 293T cells with mimics NC or miR-26a mimics (both from GenePharma Co., Ltd., Shanghai, China). After 48-h transfection, the

cells were collected and lysed, the firefly and renilla luciferase activities were detected by luciferase detection kits (Promega Corporation, Madison, WI, USA) and an ultramicro ultraviolet photometer (Bio-Rad Laboratories, Hercules, CA, USA).

Statistical analysis

All data analyses were conducted using SPSS 21.0 software (IBM Corp. Armonk, NY, USA). The measurement data conforming to the normal distribution were expressed as mean ± standard deviation. The t-test was performed for comparisons between two groups and one-way analysis of variance (ANOVA) was used for comparisons among multiple groups, Tukey's post hoc test was used for pairwise comparisons after one-way ANOVA. P value < 0.05 was indicative of statistically significant difference.

Results

Morphology of bone tissues in the SONFH group and the control group

It could be observed through HE staining that in the SONFH group, trabeculae were attenuated, scattered, and discontinuous in different degrees, in which the diffused necrotic osteocytes could be observed. Necrotic bones were wrapped and replaced by hyperplastic fiber tissues, and the hematopoietic cells in the marrow cavity were markedly declined. The control group: trabeculae were attenuated, the osteocytes could be clearly observed, there were a few necrotic empty lacunae in the osteocytes, and the proliferation of hematopoietic cells in the marrow cavity was activated (Figure 1A).

EZH2 is highly expressed in SONFH tissues

According to the results of immunohistochemical staining, the positive outcomes of EZH2 were in brown, in the SONFH tissues, EZH2 was positively expressed in the osteocytes around or in the trabeculae, and the stroma of marrow cavity. In the FNF tissues, EZH2 was negatively expressed among the osteocytes, and there were a few positive expressions in the osteoblasts on the margins of trabeculae and in the stroma of marrow cavity (Figure 1B). The statistical data (Figure 1C) revealed that relative to the control group, the EZH2 positive rate was apparently heightened in the SONFH group ($P < 0.05$).

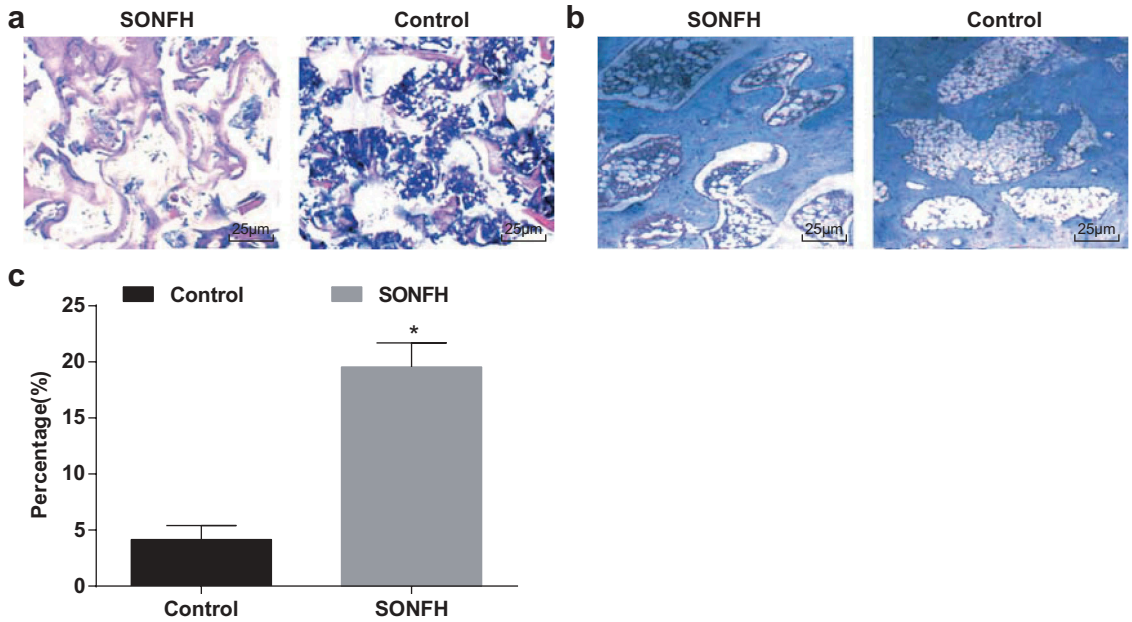

Figure 1. Morphology of bone tissues in the SONFH group and the control group. A, histological observation of the SONFH group and the control group; B, immunohistochemical staining was used to evaluate EZH2 protein in the SONFH group and the control group; C, EZH2 positive rate of the SONFH group and the control group; * $P< 0.05$ *vs* the control group; n = 30 in the control group, n = 52 in the SONFH group, the measurement data conforming to the normal distribution were expressed as mean ± standard deviation and the t-test was performed for comparisons between two groups.

miR-26a is poorly expressed and EZH2 is highly expressed in SONFH tissues

The expression of miR-26a and EZH2 in the control group and the SONFH group was determined by RT-qPCR and Western blot analysis, the outcomes of which indicated that relative to the control group, miR-26a expression was evidently reduced, and EZH2 expression was markedly elevated in the bone tissues of the SONFH group ($P < 0.05$, Figure 2A–D). These results implied that miR-26a and EZH2 may be related to SONFH, and there may exist a negative correlation.

EZH2 is the target gene of miR-26a

The target relation between miR-26a and EZH2 has been clarified by the bioinformatics software (http://www.targetscan.org, Figure 3A). The outcomes of which revealed that the luciferase activity of the EZH2-3′UTR-WT in the miR-26a mimics group was obviously abated in contrast to the mimics NC group ($P < 0.01$). While in the MUT, no apparent difference in the luciferase activity of the EZH2-3′UTR-MUT could be found between the miR-26a mimics group and the mimics NC group ($P > 0.05$, Figure 3B).

General conditions of the rats

All the rats were survived, and appeared shiver, cower, abated diet, activity, and mental state on the 1st and 2nd days after injected with Escherichia coli endotoxin. The above-mentioned symptoms were disappeared after the rats were injected with methylprednisolone for 1 w, the activity and diet of the rats were returned to normal, and there was no evident difference in the load of the limbs. After 8 weeks, rats in the SONFH groups were all appeared mild claudication, especially in the model group, the agomir NC group, the si-NC group, the miR-26a agomir + oe-EZH2 group.

Elevated miR-26a and reduced EZH2 decline blood viscosity, blood lipid, and inflammation reaction in rats with SONFH

The outcomes of hemorheology detection suggested that in contrast to the normal group, the

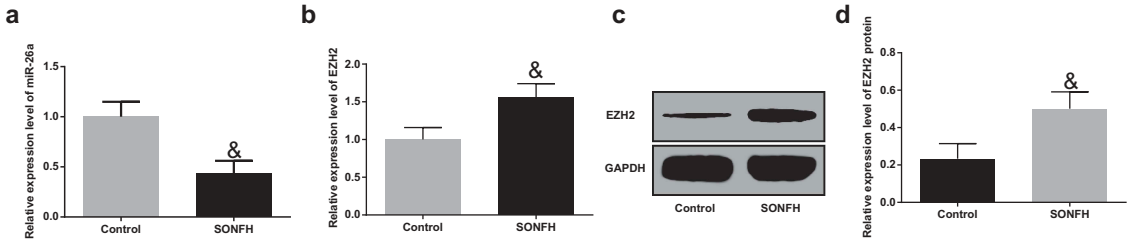

Figure 2. MiR-26a is poorly expressed and EZH2 is highly expressed in SONFH tissues. A, the expression of miR-26a in the SONFH group and the control group; B, the mRNA expression of EZH2 in bone tissues of the SONFH group and the control group; C, protein band of EZH2 in bone tissues of the SONFH group and the control group; D, the statistical results of protein expression of EZH2 in the SONFH group and the control group. & $P < 0.05$ *vs* the control group; n = 30 in the control group, n = 52 in the SONFH group, the measurement data conforming to the normal distribution were expressed as mean ± standard deviation and the t-test was performed for comparisons between two groups.

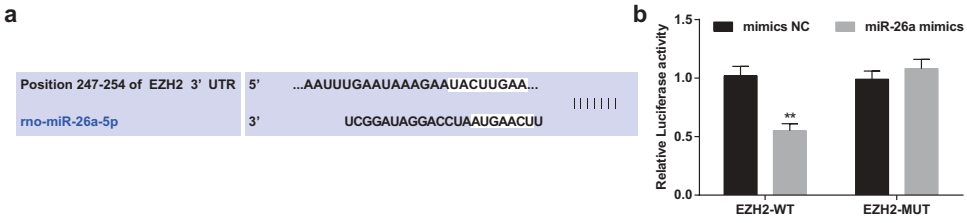

Figure 3. EZH2 is the target gene of miR-26a. A, the binding sites of miR-26a and EZH2 were predicted by online prediction software; B, the target relationship between miR-26a and EZH2 was confirmed by dual-luciferase reporter gene assay. ** $P < 0.01$ *vs* the mimics NC group; N = 3, the measurement data conforming to the normal distribution were expressed as mean ± standard deviation and the t-test was performed for comparisons between two groups.

hemorheology indices of rats in the model group were apparently heightened; compared to the agomir NC group, hemorheology indices of rats in the miR-26a agomir were broadly declined; in contrast to the si-NC group, hemorheology indices of rats in the si-EZH2 were considerably lowered; relative to the miR-26a agomir + oe-NC group, hemorheology indices of rats in the miR-26a agomir + oe-EZH2 group were markedly increased (all $P< 0.05$, Figure 4A–C).

According to the outcomes of blood lipid determination, the levels of CHO, TG, and vLDL of rats in the model group were all elevated, which was contrasted to the normal group; in comparison to the agomir NC group, levels of CHO, TG, and vLDL of rats in the miR-26a agomir group were decreased; relative to the si-NC group, levels of CHO, TG, and vLDL of rats in the si-EZH2 group were reduced; compared to the miR-26a agomir + oe-NC group, levels of CHO, TG, and vLDL of rats in the miR-26a agomir + oe-EZH2 group were heightened (all $P< 0.05$, Figure 4D).

The results of the measurement of inflammatory factors IL-6, TNF-α, and IL-1β unraveled that contrasted to the normal group, the levels of IL-6, TNF-α and IL-1β were obviously increased in the model group; relative to the agomir NC group, levels of IL-6, TNF-α and IL-1β were markedly declined in the miR-26a agomir group; in comparison to the si-NC group, levels of IL-6, TNF-α and IL-1β were broadly abated in the si-EZH2 group; in contrast to the miR-26a agomir + oe-NC group, levels of IL-6, TNF-α, and IL-1β in the miR-26a agomir + oe-EZH2 group were apparently elevated (all $P < 0.05$, Figure 4E).

Elevated miR-26a and reduced EZH2 repress the development of SONFH

In the FH sections of rats in the normal group, trabeculae were clear, and in regular arrangement; osteocytes in bone cortex and trabeculae were apparent, in which the nuclei were large and located in the center; there were osteocytes filled in the bone lacuna, and calcification zone was in well connection with subchondral trabeculae. While in the model group, the agomir NC group, the si-NC group, and the miR-26a agomir + oe-EZH2 group, trabeculae were scattered and attenuated, even ruptured, the structures were disordered, and fragment could

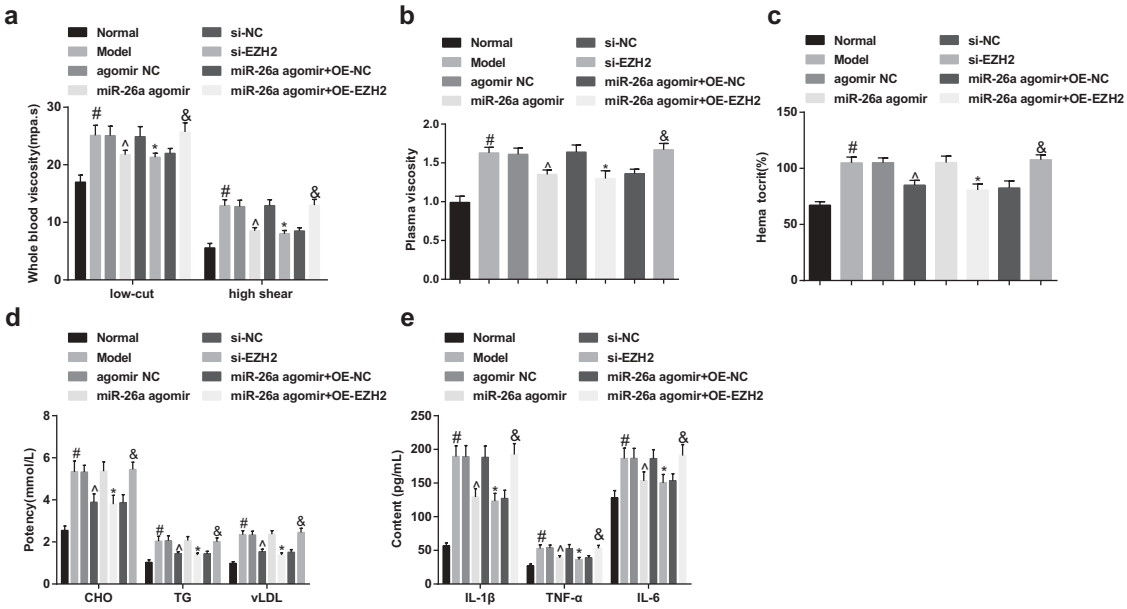

Figure 4. Elevated miR-26a and reduced EZH2 decline blood viscosity, blood lipid, and inflammation reaction in rats with SONFH. A, the comparisons of whole blood viscosity (at high and low shear) of rats among the groups; B, the comparisons of plasma viscosity of rats among the groups; C, the comparisons of hematocrit of rats among the groups; D, the comparisons of CHO, TG, and vLDL of rats among the groups; E, the comparisons of IL-1β, TNF-α, and IL-6 of rats among the groups. # P <0.05 *vs* the normal group; ^ P <0.05 *vs* the agomir NC group; * P <0.05 *vs* the si-NC group; & P <0.05 *vs* the miR-26a agomir + oe-NC group; n = 12, the measurement data conforming to the normal distribution were expressed as mean ± standard deviation, one-way ANOVA was used for comparisons among multiple groups and Tukey's post hoc test was used for pairwise comparisons after one-way ANOVA.

be found in the trabeculae. There were some necrotic osteocytes in bine lacuna and a lot of empty lacuna without osteocytes. Proliferation of fibrosis and granulation tissues was found to wrap around the trabeculae. Relative to the model group, trabeculae in the miR-26a agomir group, miR-26a agomir + oe-NC group and the si-EZH2 group were increased and became coarser, which were in clear structure. There were osteocytes filled in the bone lacuna, while a few necrotic osteocytes could be found, and the number of empty lacuna was reduced (Figure 5A).

The results of the measurement of empty lacuna rate, lacuna area, and trabeculae area indicated that compared with the normal group, empty lacuna rate, and lacuna area were evidently amplified, and trabeculae area was significantly declined in the model group; in contrast to the agomir NC group, empty lacuna rate, and lacuna area were obviously abated, and trabeculae area was broadly elevated in the miR-26a agomir group; relative to the si-NC group, empty lacuna rate and lacuna area were markedly reduced, and trabeculae area was considerably heightened in the si-EZH2 group; contrasted to the miR-26a agomir + oe-NC group, empty lacuna rate, and lacuna area were apparently increased, and trabeculae area was definitely abated in the miR-26a agomir + oe-EZH2 group (all $P < 0.05$, Figure 5B–D).

According to the outcomes of transmission electron microscope observation, osteocytes in the normal group were abundant and in normal morphology, which were in the same shape with bone lacuna. Processes in the cytoplasm were obvious and stretched into the bone canaliculus. The nuclei were large and accompanied with clear and even chromatin, there were abundant organelles, and lipid droplets could not be found. Moreover, there were plenty of bone interstitium and canaliculus, and clear fibril of bone collagen. In the model group, the agomir NC group, the si-NC group, and the miR-26a agomir + oe-EZH2 group, osteocytes were scattered and shrunk, the processes of cytoplasm were not evident. With karyopyknosis, margination, and hyperchromatism of cytoplasm could be observed in the nuclei, the perinuclear space was widened, organelles in cytoplasm were decreased, swelling of mitochondria, increased Golgi apparatus and no lipid droplet could be found. Furthermore, there were few bone interstitium and canaliculus, as well as the scattered fibril of collagen. In the miR-26a agomir + oe-NC group, the miR-26a agomir group and the si-EZH2 group, there were plentiful osteocytes, mild margination, and hyperchromatism in cytoplasm. Many organelles, a few swelled mitochondria and no lipid droplet could be discovered in cytoplasm. Bone interstitium and canaliculus were mildly widened, and fibrils of bone collagen were clear (Figure 5E).

Elevated miR-26a and reduced EZH2 up-regulate OPG expression and suppress OPGL expression in rats with SONFH

The outcomes of immunohistochemical staining revealed that there were many OPG brown-yellow particles and few OPGL brown-yellow particles could be found in the normal group. In the model group, the agomir NC group, the si-NC group, and the miR-26a agomir + oe-EZH2 group, there were a few OPG brown-yellow particles and apparently increased OPGL brown-yellow particles; and in the miR-26a agomir + oe-NC group, the miR-26a agomir group, and the si-EZH2 group, there were more OPG brown-yellow particles and relatively reduced OPGL brown-yellow particles (Figure 6A–B). In contrast to the normal group, the positive rate of OPG was noticeably lowered, and that of OPGL was remarkably elevated in the model group; relative to the agomir NC group, the positive rate of OPG was apparently heightened, and that of OPGL was broadly declined in the miR-26a agomir group; in comparison to the si-NC group, the positive rate of OPG was substantially increased, and that of OPGL was definitely lowered in the si-EZH2 group; compared with the miR-26a agomir + oe-NC group, the positive rate of OPG was noticeably reduced, and that of OPGL was markedly elevated in the miR-26a agomir + oe-EZH2 group (all $P< 0.05$, Figure 6C).

Elevated miR-26a and reduced EZH2 increase osteoblasts and decrease osteoclasts in rats with SONFH

The positive result of osteoblasts in ALP staining performed as brown, and the positive result of osteoclasts in TRAP staining performed as dark red. In the normal group, the positive osteoblasts in ALP staining

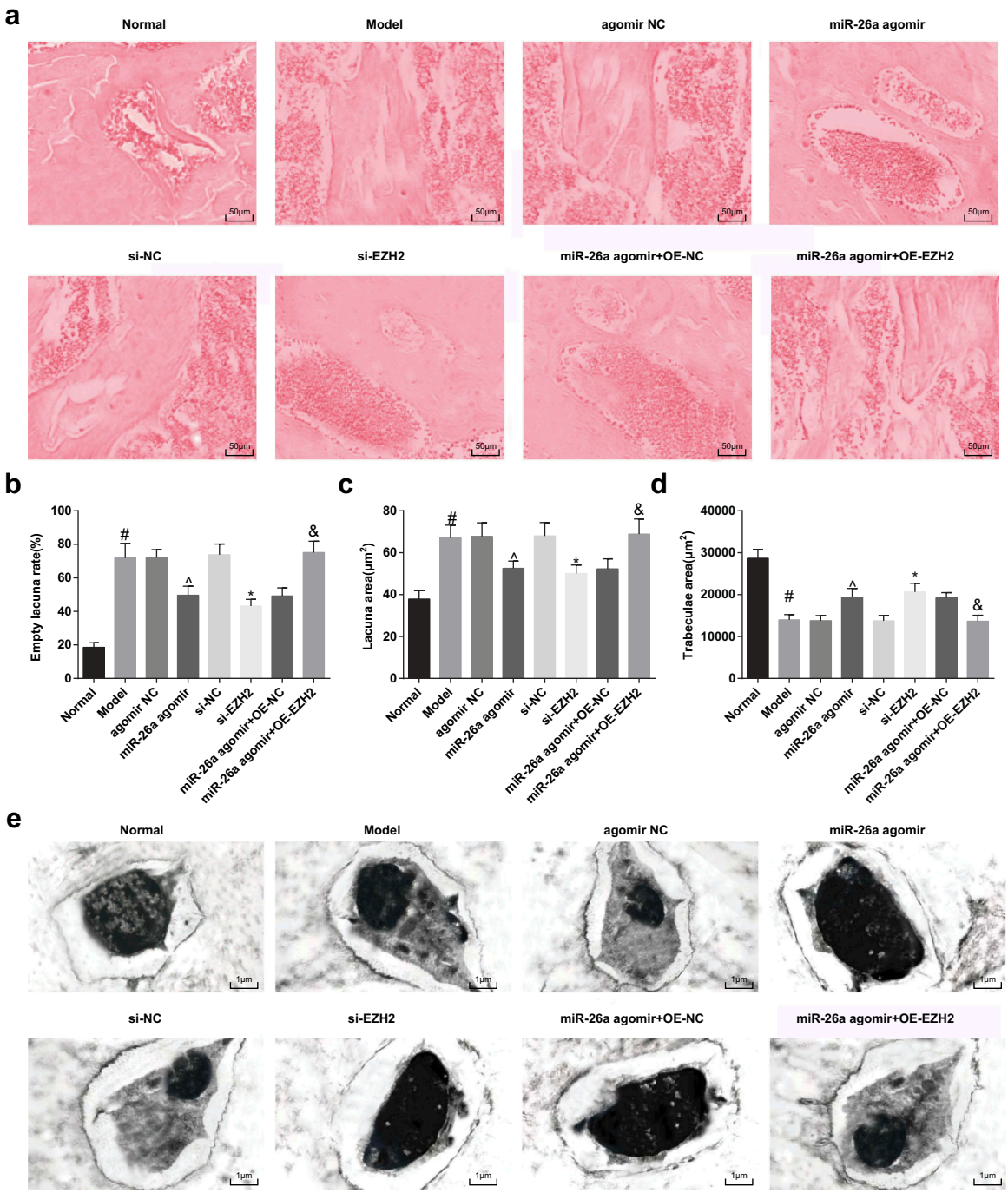

Figure 5. Elevated miR-26a and reduced EZH2 repress the development of SONFH. A, representative images of HE staining; B, the comparisons of empty lacuna rate of rats among the groups; C, the comparisons of lacuna area of rats among the groups; D, the comparisons of trabeculae area of rats among the groups; E, the results of electron microscopy observation of the FHs of rats in each group. # $P < 0.05$ *vs* the normal group; ^ $P < 0.05$ *vs* the agomir NC group; * $P < 0.05$ *vs* the si-NC group; & $P < 0.05$ *vs* the miR-26a agomir + oe-NC group; n = 12, the measurement data conforming to the normal distribution were expressed as mean ± standard deviation, one-way ANOVA was used for comparisons among multiple groups and Tukey's post hoc test was used for pairwise comparisons after one-way ANOVA.

were in round form, presented a gathering pattern, and distributed in trabecular space of marrow cavity and the surface of trabeculae; osteoclasts in TRAP staining were not of uniform size, which were fusiform, and the osteoclasts were evenly distributed around trabeculae; the positive osteoblasts in the

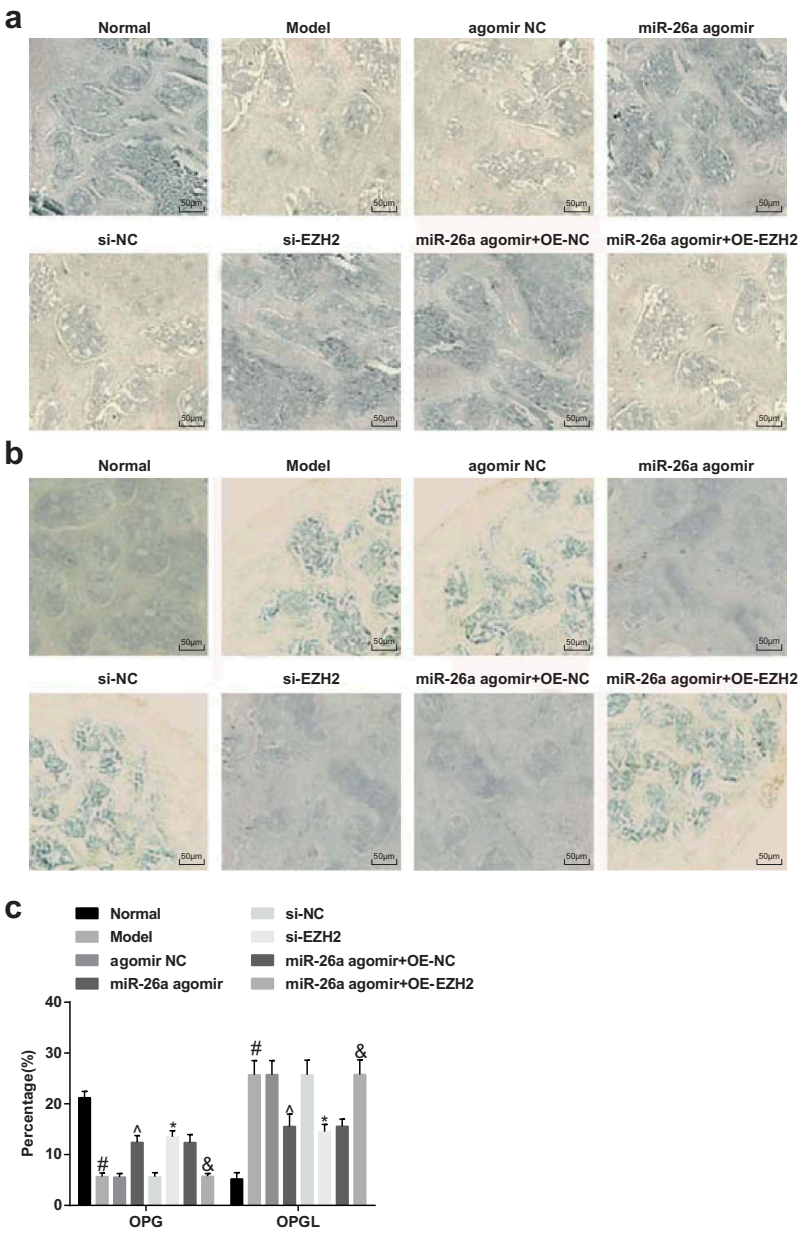

Figure 6. Elevated miR-26a and reduced EZH2 up-regulate OPG expression and suppress OPGL expression in rats with SONFH. A, representative images of OPG of rats in each group in immunohistochemical staining; B, representative images of OPGL of rats in each group in immunohistochemical staining; C, the positive rates of OPG and OPGL of rats in each group, # $P < 0.05$ *vs* the normal group; ^ $P < 0.05$ *vs* the agomir NC group. * $P < 0.05$ *vs* the si-NC group; & $P < 0.05$ *vs* the miR-26a agomir + oe-NC group; n = 12, the measurement data conforming to the normal distribution were expressed as mean ± standard deviation, one-way ANOVA was used for comparisons among multiple groups and Tukey's post hoc test was used for pairwise comparisons after one-way ANOVA.

model group, agomir NC group, the si-NC group, the miR-26a agomir + oe-EZH2 group were diffusely distributed in trabecular space of marrow cavity; the positive osteoclasts were increased and mainly in polygon, which were multinuclear; in the miR-26a agomir + oe-NC group, the miR-26a agomir group and the si-EZH2 group, positive osteoblasts were diffusely distributed in trabecular space of marrow cavity and the surface of some trabeculae, positive osteoclasts were smaller and strip-like, which were in regular morphology (Figure 7A–B).

The numbers of positive osteoclasts and osteoblasts were calculated by an image analyzer, the results implied that compared with the normal group, the

number of positive osteoblasts was reduced, and that of positive osteoclasts was elevated in the model group; relative to the agomir NC group, the number of positive osteoblasts was increased, and that of positive osteoclasts was declined in the miR-26a agomir group; in contrast to the si-NC group, the number of positive osteoblasts was amplified, and that of positive osteoclasts was repressed in the si-EZH2 group; in comparison to the miR-26a agomir + oe-NC group, the number of positive osteoblasts was decreased, and that of positive osteoclasts was increased in the miR-26a agomir + oe-EZH2 group (all $P < 0.05$, Figure 7C).

Elevated miR-26a and reduced EZH2 decelerate the apoptosis of osteocytes in SONFH rats

Western blot analysis was employed to determine the protein expression of Bax and Bcl-2 in FH tissues of rats in each group, the outcomes of which indicated that in comparison to the normal group, the protein expression of Bax was significantly elevated, and the protein expression of Bcl-2 was evidently reduced in the model group; contrasted to the agomir NC group, the protein expression of Bax was broadly lowered, and the protein expression of Bcl-2 was apparently

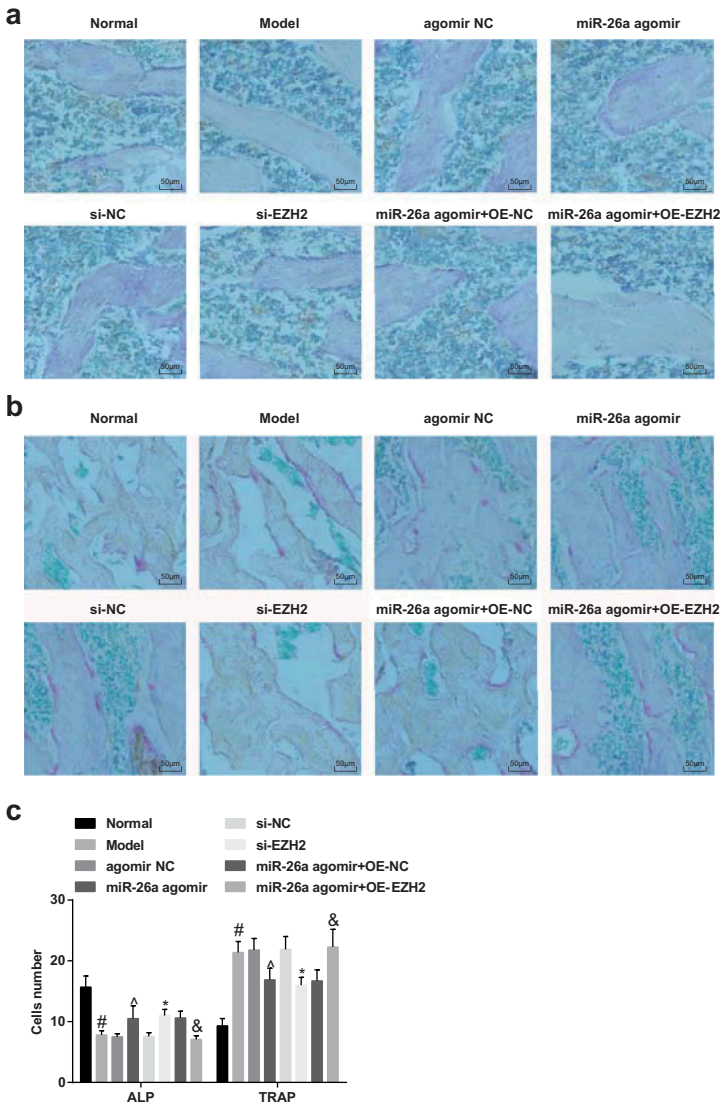

Figure 7. Elevated miR-26a and reduced EZH2 increase osteoblasts and decrease osteoclasts in rats with SONFH. A, representative images of osteoblasts of rats in each group in ALP staining; B, representative images of osteoclasts of rats in each group in TRAP staining; C, the numbers of positive osteoblasts and osteoclasts, respectively, in ALP staining and TRAP staining. # P <0.05 *vs* the normal group; ^ P <0.05 *vs* the agomir NC group; * P <0.05 *vs* the si-NC group; & P <0.05 *vs* the miR-26a agomir + oe-NC group; n = 12, the measurement data conforming to the normal distribution were expressed as mean ± standard deviation, one-way ANOVA was used for comparisons among multiple groups and Tukey's post hoc test was used for pairwise comparisons after one-way ANOVA.

heightened in the miR-26a agomir group; relative to the si-NC group, the protein expression of Bax was considerably abated, and the protein expression of Bcl-2 was markedly amplified in the si-EZH2 group; in contrast to the miR-26a agomir + oe-NC group, the protein expression of Bax was significantly elevated, and the protein expression of Bcl-2 was evidently declined in the miR-26a agomir + oe-EZH2 group (all $P< 0.05$, Figure 8A–C), implying that the up-regulated miR-26a could attenuate the apoptosis of osteocytes in SONFH bone tissues by promoting the expression of Bcl-2 and repressing the expression of Bax.

The results of TUNEL assay suggested that compared with the normal group, the apoptotic rate of the model group was elevated; in contrast to the agomir NC group, the apoptotic rate of the miR-26a agomir group was abated; relative to the si-NC group, the apoptotic rate of the si-EZH2 group was lowered; contrasted to the miR-26a agomir + oe-NC group, the apoptotic rate of the miR-26a agomir + oe-EZH2 group was heightened (all $P< 0.05$, Figure 8D), indicating that the elevation of miR-26a or the knockdown of EZH2 could decelerate the apoptosis of osteocytes in SONFH rats, and up-regulated miR-26a could ameliorate the FH injury and apoptosis of osteocytes in SONFH rats by suppressing EZH2.

miR-26a is down-regulated while EZH2 is up-regulated in FH tissues of SONFH rats

The expression of miR-26a and EZH2 was evaluated by RT-qPCR and Western blot analysis, the outcomes showed that in comparison to the normal group, miR-26a was poorly expressed, and EZH2 was highly expressed in the model group; contrast to the agomir NC group, miR-26a was up-regulated, and EZH2 was down-regulated in the miR-26a agomir group (both $P < 0.05$); there was no evident difference in the expression of miR-26a between the si-NC group and the si-EZH2 group ($P > 0.05$), and EZH2 expression was markedly suppressed in the si-EZH2 group ($P < 0.05$); no apparent difference could

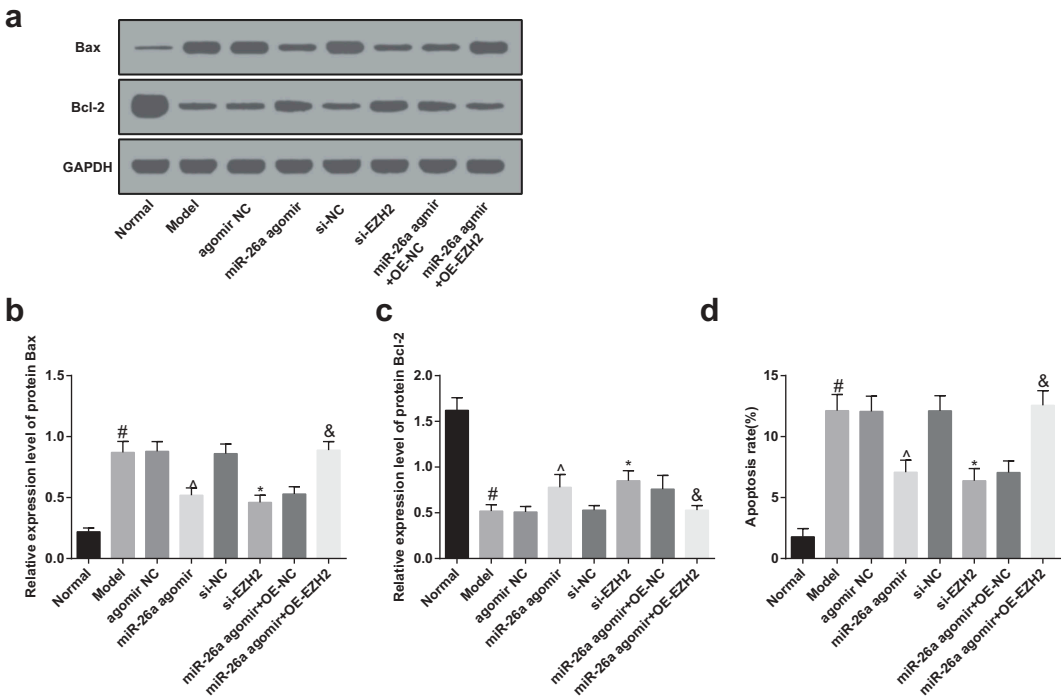

Figure 8. Elevated miR-26a and reduced EZH2 decelerate the apoptosis of osteocytes in SONFH rats. A, protein bands of Bax and Bcl-2 in FH tissues of rats in each group; B, the comparisons of Bax protein expression of FH tissues in rats among the groups; C, the comparisons of Bcl-2 protein expression of FH tissues in rats among the groups; D, the comparisons of apoptotic rate of osteocytes in rats among the groups. # P <0.05 *vs* the normal group; ^ P <0.05 *vs* the agomir NC group; * P <0.05 *vs* the si-NC group; & P <0.05 *vs* the miR-26a agomir + oe-NC group; n = 12, the measurement data conforming to the normal distribution were expressed as mean ± standard deviation, one-way ANOVA was used for comparisons among multiple groups and Tukey's post hoc test was used for pairwise comparisons after one-way ANOVA.

be found in the expression of miR-26a between the miR-26a agomir + oe-NC group and the miR-26a agomir + oe-EZH2 group ($P > 0.05$), and the expression of EZH2 was noticeably elevated in the miR-26a agomir + oe-EZH2 group ($P < 0.05$, Figure 9A–C).

Discussion

Resulted from usage of glucocorticoid, SONFH is a severe complication that may cause osteoporotic fractures as well as aseptic necrosis of FH [22]. Moreover, the miRNAs were proved to play a vital role in leading molecules in the RNA silencing [23]. In addition, there were some studies have clarified that the functions of miR-26a might be associated with human diseases, such as human osteosarcoma [24] and osteoarthritis [25]. However, there is little known about the function mechanisms of miR-26a as well as its target gene EZH2 in SONFH. Consequently, this study was designed to probe into the regulative impacts of miR-26a and EZH2 on SONFH, and we have found in our study that the up-regulation of miR-26a and knockdown of EZH2 could suppress the development of SONFH.

Among the essential results of our study, one of them demonstrated that miR-26a was poorly expressed in SONFH, indicating that there was an abnormal expression of miR-26a in SONFH. The aberrant performance of miR-26a has also been identified in other studies. For instance, Chen *et al.* have unearthed in their research that miR-26a was down-regulated in cartilage tissues and inflammatory articular chondrocytes in rheumatoid arthritis [26]. What's more, the reduction of miR-26a has been found in prostate cancer as well [27]. Another finding in our research suggested that EZH2 exerted an up-regulation in SONFH. In accordance with this finding, the elevation of EZH2 has also been clarified in human and murine melanoma by Daniel Zingg *et al.* [28]. Subsequently, the target relation between miR-26a and EZH2 has been discovered in our study, which implied that EZH2 was a target gene of miR-26a. Consistent with this outcome, EZH2 has been found to be a direct target of miR-26a in hepatocellular carcinoma cells [19] and nasopharyngeal carcinoma [20].

In addition, we have also found that the elevation of miR-26a and knockdown of EZH2 were able to abate the inflammatory reaction in SONFH. Similar with this result, Xie *et al.* have found that the down-regulation of miR-26a was associated with elevated chronic inflammation in chondrocytes, and the reciprocal prohibition between miR-26a and nuclear factor-kappa B could modulate the obesity-related chronic inflammation in chondrocytes [29]. Besides, EZH2 has been reported to be able to regulate the inflammation of nonalcoholic fatty liver disease *in vivo* and *in vitro* [30]. Another finding in our research revealed that the up-regulation of miR-26a and the down-regulation of EZH2 could attenuate the progression of SONFH and the injury that is induced by SONFH. In line with this result, the protective role of EZH2 in acute kidney injury that is induced by ischemia and reperfusion has been confirmed by Liang *et al.* [31]. According to a recent research, the overexpression of miR-26a has the capacity to protect neural stem cells from

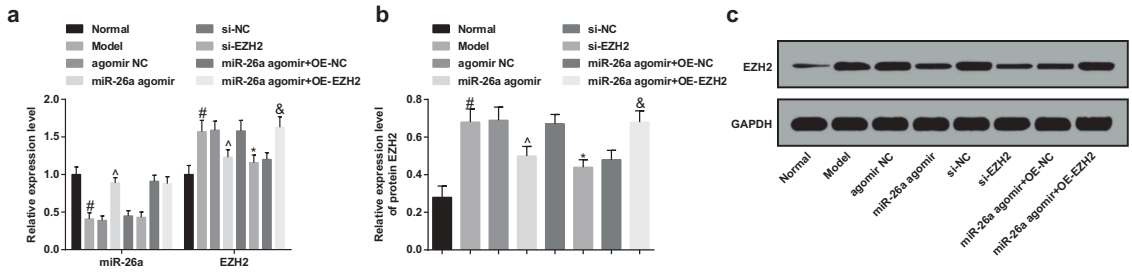

Figure 9. MiR-26a is down-regulated while EZH2 is up-regulated in FH tissues in rats with SONFH. A, comparisons of miR-26a and EZH2 expression in FH tissues of rats among the groups; B, comparisons of protein expression of EZH2 in FH tissues of rats among the groups; C, protein band of EZH2 in rats' FH tissues of each group. # P <0.05 *vs* the normal group; ^ P <0.05 *vs* the agomir NC group; * P <0.05 *vs* the si-NC group; & P <0.05 *vs* the miR-26a agomir + oe-NC group; n = 12, the measurement data conforming to the normal distribution were expressed as mean ± standard deviation, one-way ANOVA was used for comparisons among multiple groups and Tukey's post hoc test was used for pairwise comparisons after one-way ANOVA.

cardiac arrest-induced brain damage by the activation of the β-catenin signaling pathway [32]. Moreover, we have found that the elevated miR-26a and restrained EZH2 could ameliorate the apoptosis of osteoblasts in SONFH by repressing Bax and elevating Bcl-2. Similar to our result, an extant literature has pointed out that the expression of miR-26a was in negative correlation with the level of Bax in glioblastoma multiform [33]. There was another study has discovered that miR-26a could protect type II alveolar epithelial cells from mitochondrial apoptosis by regulating the levels of Bax and Bcl-2 in acute respiratory distress syndrome [34]. Additionally, Yu *et al*. have found that the restrained EZH2 was able to repress the apoptosis in nasopharyngeal carcinoma cells [35]. All the literatures were helpful to the diagnosis and treatment of SONFH, as well as the molecule mechanisms of miRNAs.

In conclusion, this research suggests that miR-26a was degraded, and EZH2 was highly expressed in SONFH. Moreover, this study confirmed the hypothesis that the elevation of miR-26 could play a protective role in osteocyte injury induced by SONFH via repressing the expression of EZH2, and also could repress the development of SONFH by restraining the inflammation and the apoptosis of osteocytes. Nevertheless, more endeavors remain to further explore the function of miR-26a and EZH2 in the development of SONFH.

Acknowledgments

We would like to acknowledge the reviewers for their helpful comments on this paper.

Authors' contributions

Guarantor of integrity of the entire study: Gang Li
Study design: HaiFeng Liu, QingHe Liu
Experimental studies: XiaoGang Zhang, XingChao Liu
Manuscript editing: GuoDong Zhang

Disclosure statement

No potential conflict of interest was reported by the authors.

Ethical statement

Written informed consents were obtained from all patients prior to the study. The protocols of this study were approved by the Ethics Committee of Beijing Chaoyang Hospital, Capital Medical University and based on the ethical principles for medical research involving human subjects of the Helsinki Declaration. Animal experiments were strictly in accordance with the Guide to the Management and Use of Laboratory Animals issued by the National Institutes of Health. The protocol of animal experiments was approved by the Institutional Animal Care and Use Committee of Beijing Chaoyang Hospital, Capital Medical University.

Funding

This work was supported by The Key scientific and technological research programs of HeBei Province, Grant/Award Number: 20180897; The Key scientific and technological research programs of HeBei Province [20180897].

References

[1] Zhao D, Cui D, Wang B, et al. Treatment of early stage osteonecrosis of the femoral head with autologous implantation of bone marrow-derived and cultured mesenchymal stem cells. Bone. 2012;50(1):325–330.
[2] Li Z, Jiang C, Li X, et al. Circulating microRNA signature of steroid-induced osteonecrosis of the femoral head. Cell Prolif. 2018;51(1):e12418.
[3] Aimaiti A, Wufuer M, Wang Y-H, et al. Can bisphenol A diglycidyl ether (BADGE) administration prevent steroid-induced femoral head osteonecrosis in the early stage? Med Hypotheses. 2011;77(2):282–285.
[4] Song Y, Du Z, Ren M, et al. Association of gene variants of transcription factors PPARgamma, RUNX2, Osterix genes and COL2A1, IGFBP3 genes with the development of osteonecrosis of the femoral head in Chinese population. Bone. 2017;101:104–112.
[5] Tian Y, An F, Wang J, et al. MMP2 and MMP10 polymorphisms are related to steroid-induced osteonecrosis of the femoral head among Chinese Han population. Biomed Res Int. 2019;2019:8298193.
[6] Bai R, LIU W, ZHAO A, et al. Nitric oxide content and apoptosis rate in steroid-induced avascular necrosis of the femoral head. Exp Ther Med. 2015;10(2):591–597.
[7] Lin Z, Lin Y. Identification of potential crucial genes associated with steroid-induced necrosis of femoral head based on gene expression profile. Gene. 2017;627:322–326.
[8] Yang IP, Tsai H-L, Hou M-F, et al. MicroRNA-93 inhibits tumor growth and early relapse of human colorectal cancer by affecting genes involved in the cell cycle. Carcinogenesis. 2012;33(8):1522–1530.
[9] Hao C, Yang S, Xu W, et al. MiR-708 promotes steroid-induced osteonecrosis of femoral head, suppresses osteogenic differentiation by targeting SMAD3. Sci Rep. 2016;6:22599.

[10] Gu C, Xu Y, Zhang S, et al. miR-27a attenuates adipogenesis and promotes osteogenesis in steroid-induced rat BMSCs by targeting PPARgamma and GREM1. Sci Rep. 2016;6:38491.
[11] Wang Z, Wang Z, Liu J, et al. Long non-coding RNA SNHG5 sponges miR-26a to promote the tumorigenesis of osteosarcoma by targeting ROCK1. Biomed Pharmacother. 2018;107:598–605.
[12] Liu J, Mi B, Wang Y, et al. miR-26a suppresses osteosarcoma migration and invasion by directly targeting HMGA1. Oncol Lett. 2018;15(6):8303–8310.
[13] Li Z, Ni J. Role of microRNA-26a in the diagnosis of lower extremity deep vein thrombosis in patients with bone trauma. Exp Ther Med. 2017;14(5):5069–5074.
[14] Zhao Z, Dai XS, Wang ZY, et al. MicroRNA-26a reduces synovial inflammation and cartilage injury in osteoarthritis of knee joints through impairing the NF-kappaB signaling pathway. Biosci Rep. 2019;39:4.
[15] McCabe MT, Ott HM, Ganji G, et al. EZH2 inhibition as a therapeutic strategy for lymphoma with EZH2-activating mutations. Nature. 2012;492(7427):108–112.
[16] Sun R, Shen J, Gao Y, et al. Overexpression of EZH2 is associated with the poor prognosis in osteosarcoma and function analysis indicates a therapeutic potential. Oncotarget. 2016;7(25):38333–38346.
[17] Huo Y, Li Q, Wang X, et al. MALAT1 predicts poor survival in osteosarcoma patients and promotes cell metastasis through associating with EZH2. Oncotarget. 2017;8(29):46993–47006.
[18] Adamik J, Jin S, Sun Q, et al. EZH2 or HDAC1 inhibition reverses multiple myeloma-induced epigenetic suppression of osteoblast differentiation. Mol Cancer Res. 2017;15(4):405–417.
[19] Zhuang C, Wang P, Huang D, et al. A double-negative feedback loop between EZH2 and miR-26a regulates tumor cell growth in hepatocellular carcinoma. Int J Oncol. 2016;48(3):1195–1204.
[20] Lu J, He M-L, Wang L, et al. MiR-26a inhibits cell growth and tumorigenesis of nasopharyngeal carcinoma through repression of EZH2. Cancer Res. 2011;71(1):225–233.
[21] Dong YL, Zhou L, Li Y-L, et al. Establishment and assessment of rat models of glucocorticoid-induced osteonecrosis. Zhongguo Yi Xue Ke Xue Yuan Xue Bao. 2015;37(2):152–156.
[22] Xu X, Wen H, Hu Y, et al. STAT1-caspase 3 pathway in the apoptotic process associated with steroid-induced necrosis of the femoral head. J Mol Histol. 2014;45(4):473–485.
[23] Ha M, Kim VN. Regulation of microRNA biogenesis. Nat Rev Mol Cell Biol. 2014;15(8):509–524.
[24] Taheriazam A, Bahador R, Karbasy SH, et al. Down-regulation of microRNA-26a and up-regulation of microRNA-27a contributes to aggressive progression of human osteosarcoma. Diagn Pathol. 2015;10:166.
[25] Shen H, Wang Y, Shi W, et al. LncRNA SNHG5/miR-26a/SOX2 signal axis enhances proliferation of chondrocyte in osteoarthritis. Acta Biochim Biophys Sin (Shanghai). 2018;50(2):191–198.
[26] Jiang L, Cao S. Role of microRNA-26a in cartilage injury and chondrocyte proliferation and apoptosis in rheumatoid arthritis rats by regulating expression of CTGF. J Cell Physiol. 2020;235(2):979–992.
[27] Mohammadi Torbati P, Asadi F, Fard-Esfahani P. Circulating miR-20a and miR-26a as biomarkers in prostate cancer. Asian Pac J Cancer Prev. 2019;20(5):1453–1456.
[28] Zingg D, Debbache J, Schaefer SM, et al. The epigenetic modifier EZH2 controls melanoma growth and metastasis through silencing of distinct tumour suppressors. Nat Commun. 2015;6:6051.
[29] Xie Q, Wei M, Kang X, et al. Reciprocal inhibition between miR-26a and NF-kappaB regulates obesity-related chronic inflammation in chondrocytes. Biosci Rep. 2015;35(3). DOI:10.1038/ncomms7051.
[30] Vella S, Gnani D, Crudele A, et al. EZH2 down-regulation exacerbates lipid accumulation and inflammation in in vitro and in vivo NAFLD. Int J Mol Sci. 2013;14(12):24154–24168.
[31] Liang H, Huang Q, Liao M-J, et al. EZH2 plays a crucial role in ischemia/reperfusion-induced acute kidney injury by regulating p38 signaling. Inflamm Res. 2019;68(4):325–336.
[32] Li F, Wei H, Li H, et al. miR-26a prevents neural stem cells from apoptosis via beta-catenin signaling pathway in cardiac arrest-induced brain damage. Biosci Rep. 2019;39(5):BSR20181635.
[33] Ge X, Pan M-H, Wang L, et al. Hypoxia-mediated mitochondria apoptosis inhibition induces temozolomide treatment resistance through miR-26a/Bad/Bax axis. Cell Death Dis. 2018;9(11):1128.
[34] Xu BY, Li Y-L, Luan B, et al. MiR-26a protects type II alveolar epithelial cells against mitochondrial apoptosis. Eur Rev Med Pharmacol Sci. 2018;22(2):486–491.
[35] Yu M, Li Y, Li M, et al. Eudesmin exerts antitumor effects by down-regulating EZH2 expression in nasopharyngeal carcinoma cells. Chem Biol Interact. 2019;307:51–57.